Evaluating the effects of the Prime Location Housing Reform on Housing Demand in Singapore

Masters Thesis: Columbia University

Naia Nathan*

December 11, 2025

Abstract

This paper evaluates Singapore's November 2021 Prime Location Housing (PLH) reform, which restricted resale profitability of centrally-located public housing to reduce speculative demand. To separate demand effects from supply, I develop an equilibrium model of the Build-to-Order lottery system showing that changes in application rates reveal changes in household valuations. The treated group (prime properties) differs systematically from the control group, causing unconditional parallel trends testing to fail, and precluding use of conventional DiD. Hence, I employ Causal Forest Difference-in-Differences to estimate Aggregate Treatment Effect on the Treated (ATT), which permits identification under conditional parallel trends. Using novel panel data on 493 BTO launches from 2011–2023, I estimate that the reform increased first-timer success probability by 0.50 log points ($p = 0.029$), implying a 65% level reduction in household valuations for prime locations. Placebo tests at eight pre-treatment dates yield zero significant effects, and an event study reveals treatment effects strengthening over time consistent with market learning. These findings provide the first evidence that restrictions on housing resale profitability can meaningfully dampen speculative demand in lottery allocation systems.

*Supervised by Professor Jonathan Dingel (Columbia University). With thanks to Dr Kwok-Hao Lee (National University of Singapore) and Dr Arka Bandyopadhyay (Columbia University) for advice.

Contents

1 Introduction

Singapore's housing system is unique because of its significant lottery effect. Over 80% of residents live in public housing administered by the Housing Development Board (HDB), with new units allocated primarily through a lottery system called Build-to-Order (BTO). This arrangement creates substantial windfall effects: households fortunate enough to win flats in desirable locations subsequently resell them at prices far exceeding their purchase price. Such windfalls are particularly pronounced for central public housing, where owners have realized profits exceeding 100% of their initial outlay—for example, Pinnacle@Duxton units purchased for under S$400,000 have resold for over S$1.2 million (Straits Times, 2022). The prospect of such supernormal profits has historically driven extreme oversubscription for prime location BTOs, with application rates reaching 20–30 times supply (see Appendix A).

In November 2021, the Prime Location Housing (PLH) reform was implemented. It penalized the resaleability of central public housing, aiming to reallocate demand and prevent speculative buying. This paper evaluates the policy's effectiveness in reducing oversubscription of prime location housing, and uses demand responses to provide suggestive evidence on its effects on speculative buying behavior.

Studying policy effects on housing demand is challenging because of the fundamental simultaneity between supply and demand. It is unclear whether changes in application rates reflect shifts in household valuations or changes in supply conditions. The existing literature on public housing allocation has approached this identification problem through various methods. Waldinger (2021) uses revealed preference analysis of wait list data to estimate preferences for public housing in Cambridge, Massachusetts, finding substantial heterogeneity in applicant valuations and a trade-off between efficiency and redistribution in mechanism design. Thakral (2016a) develops a structural model of the Pittsburgh public housing allocation system to evaluate alternative allocation rules. In the context of housing lotteries, Zhou (2023) studies Shanghai's presale housing market under price ceilings, estimating that waiting costs and misallocation from rationing generate substantial welfare losses. Cook et al. (2023) use a discrete choice framework to evaluate location decisions in Chicago's Low-Income Housing Tax Credit program, finding that building in higher-opportunity neighborhoods increases household welfare but shifts the distribution of assistance toward more moderate-need households.

Most directly related to this paper is the work of Lee et al. (2024), who develop a dynamic discrete choice model of Singapore's BTO allocation system. They show that households exhibit forward-looking behavior, strategically timing their applications across BTO rounds, and that increasing supply alone may fail to reduce wait times due to induced strategic delay. Building on this foundation, Ferdowsian et al. (2025) study optimal mechanism design when the planner controls both allocation rules and supply, finding that batching applications artificially generates competition and improves match quality. These papers provide the theoretical and empirical foundation for understanding household behavior in Singapore's BTO system.

To interpret changes in application rates as a measure of policy effectiveness, I develop a theoretical model in Section 3 that conceptualizes these changes as differences in valuation. Households maximize expected discounted utility by choosing a single project-room type combination each round. The value of bidding is the product of utility gained from winning and the probability of success. In equilibrium, rational households allocate across projects such that no arbitrage opportunities exist, equalizing the value of applying to any project. From this equilibrium condition, I derive an estimating equation showing how Difference-in-Differences captures the change in

valuation of prime properties after the reform.

I then apply a Causal Forest Difference-in-Differences (CF-DiD) framework to estimate the Average Treatment Effect on the Treated (ATT). CF-DiD uses random forests to orthogonalize confounders, enabling DiD estimation when the treated group differs systematically from the control group and treatment assignment is non-random, provided conditional parallel trends holds. This approach was formalized by Gavrilova et al. (2025), building on the work of Abadie (2005b), Athey et al. (2019), Wager and Athey (2018), and Chernozhukov et al. (2018).

I find evidence that the policy succeeded in reducing oversubscription of housing in prime locations, improving allocative efficiency. The estimated reduction in logarithmic probability of lottery success is 0.50 log points ($p = 0.029$, 95% CI: [0.18, 1.01]), representing approximately a 65% fall in valuation of prime properties in level terms ($e^{0.50} - 1 \approx 0.65$). This finding is validated by robustness checks recommended in the literature (Gavrilova et al., 2025; Chernozhukov et al., 2018; Athey, 2015), including conditional parallel trends and placebo tests.

These findings also provide suggestive preliminary evidence that the policy reduced speculative buying behavior. The economic model (Section 3) demonstrates that valuation changes are largely driven by reductions in expected resale profit. While definitive evidence on resale prices must await the 2031 transaction data, my results suggest that the *expectation* of resale profits has declined for prime housing, supporting restrictions on resaleability as an effective measure to reduce speculative demand.

This paper makes three contributions. First, it is the first paper to study the effects of the 2021 PLH reform. Second, it proposes a model of public housing lotteries in which application rates serve as measures of household valuation. Third, it provides the first application of a machine learning Difference-in-Differences approach to housing policy evaluation.

The remainder of the paper proceeds as follows. Section 2 provides background on Singapore's public housing system, the BTO lottery, and the 2021 reform. Section 3 presents the theoretical economic model and shows why a traditional DiD approach is infeasible, motivating the CF-DiD methodology. Section 4 explains CF-DiD and justifies its application. Section 5 describes the data and empirical implementation. Section 6 presents results and validation tests. Section 7 concludes with limitations and directions for future research.

2 Background

This section provides background on Singapore's public housing landscape, explains the design of the BTO lottery, and describes the 2021 reform.

2.1 Singapore Public Housing Context

Singapore is unusual in that over 80% of residents live in government-subsidized public housing administered by the Housing Development Board (HDB). There are two main mechanisms to obtain such a flat: through the HDB Build-to-Order (BTO) lottery or on the resale market when existing owners sell their units.

Eligibility for BTO. Unlike many subsidized housing schemes internationally, Singapore's income cap for BTO eligibility is set above the median household income. The cap is S$14,000, while median household income from work was S$10,869 in 2023 (Department of Statistics Singapore, 2024). All couples aged 21 and above with at least one Singaporean partner are eligible to apply if their household income falls below the cap. Singles are eligible only after age 35 and

face de-prioritization in the allocation of 3- to 5-room flats. The scheme is designed to support family formation, an important policy objective given Singapore's declining birth rate and aging population.

Rules of Ownership. As the name suggests, BTOs are Built-to-Order: after allocation, households typically wait 3–5 years for construction to complete before moving in (see Appendix A for historical wait times). After construction, owners must occupy the unit for a Minimum Occupancy Period (MOP) of 5 years before they may rent or sell the property. The flat lease is 99 years, after which ownership reverts to the government. Town councils comprising elected representatives are responsible for maintaining common areas.

Resale Market. The resale market for HDB flats has experienced sustained price appreciation, particularly for prime location properties. Resale prices are highest immediately after the MOP and depreciate over their 99-year term. A substantial fraction of BTO purchasers sell their units within a few years of the MOP, suggesting investment rather than owner-occupation motives. This pattern has been reinforced by the framing of property as an investment vehicle in Singapore's policy discourse and financial planning culture. Buyers on the resale market must also meet citizenship requirements and may receive government subsidies, though these are smaller than for new BTOs.

Pricing and Subsidies. HDB subsidizes BTOs in two stages: pricing units below market value at the time of sale and applying additional means-tested subsidies. Pricing is set administratively using an algorithm that the government does not disclose publicly; authorities state that prices reflect a markdown from estimated market value based on nearby resale transactions. Additional subsidies are available for specific groups—for example, low-income households and those living near parents. Pricing is regime-dependent: PLH flats receive higher initial subsidies to maintain affordability despite their central locations, with a corresponding subsidy clawback upon resale.

Pricing varies substantially across market segments. For example, in my dataset, the average price of a 4-room BTO in Bedok in 2024 was S$525,000, while the average price of a 4-room resale (with at least 90 years left on the lease) was S%820,000 in the same year. Comparable private housing would cost several times more. Given this price differential, private housing constitutes an effectively separate market for most BTO-eligible households. For tractability, the model assumes households focus primarily on the BTO market, though Lee et al. (2024) provide a more complete model incorporating resale market dynamics.

2.2 HDB BTO Lottery Design before November 2021

When demand exceeds supply, BTOs are allocated by random lottery subject to priority schemes. Priority is given to first-timer applicants (those who have not previously received housing subsidies) and to applicants living near family. This paper focuses on first-timer applicants, who constitute approximately 85% of applicants and are reserved at least 85% of 3-room flats and 95% of 4- and 5-room flats in each launch (Housing and Development Board, 2022). I exclude 2-room Flexi flats and studios, which serve senior citizens under different priority rules and likely exhibit distinct demand patterns.

Crucial to this paper is that applicants may bid on only one project-room type combination per round, creating a strategic dimension to household decision-making. Utility in this context is the product of expected utility from obtaining a flat and the probability of success—a structure

formalized in Section 3. Applicants can observe application rates in real time through a government portal that updates throughout the application window. If a property faces unexpectedly high demand, applicants may withdraw and reapply to a less competitive option within the same round.

Until 2023, there were no penalties for rejecting an allocated flat, making bidding in every round a strictly dominant strategy for all eligible households (Lee et al., 2024). Consequently, the model can assume all eligible and willing households bid each round without considering option value from future launches.

2.3 Prime Location Housing (November 2021 Reform)

The PLH model applies to properties in designated central locations. The reform imposes four key restrictions affecting resale profitability:

1. **Extended MOP**: The Minimum Occupancy Period increases from 5 years to 10 years.
2. **Rental prohibition**: Owners face a permanent ban on renting out the entire apartment.
3. **Subsidy clawback**: Upon resale, owners must return a percentage (6–9%) of the higher of resale price or valuation to HDB.
4. **Buyer restrictions**: Resale is restricted to households meeting the S$14,000 income ceiling, limiting the pool of potential buyers.

These provisions collectively reduce expected resale profits and shift BTO demand toward owner-occupation rather than investment.

2.4 Policy Regimes

Identification of the PLH reform's effects is complicated by multiple policy changes and macroeconomic shocks during the analysis period:

- **Mature vs. non-mature estates**: Different allocation quotas apply across estate classifications.
- **Rejection penalty (2023)**: Penalties for declining allocated flats were introduced, altering strategic incentives.
- **2024 Plus scheme**: A new intermediate classification was introduced between Standard and Prime flats.
- **COVID-19**: The pandemic caused sharp increases in resale prices and, through lockdowns, may have heightened demand for homeownership (lockdown occurred in 2021).

To isolate the PLH effect from these confounds, I focus on November 2021 through August 2023 as the primary analysis window, a period relatively free of major policy shocks after the PLH introduction.

2.5 What Drives BTO Demand?

The literature provides a foundation for understanding BTO demand through a hedonic pricing framework. Diao et al. (2017) document the importance of MRT accessibility for housing values, while Lee and Tan (2024) show that transit access differentially affects households across the income distribution. Lee et al. (2024) demonstrate that households exhibit forward-looking behavior, incorporating future resale values and competition into their current bidding decisions. This forward-looking structure motivates the valuation framework developed in Section 3, where current application decisions reflect discounted expected utility inclusive of future resale profits.

3 Economic Model

Understanding household responses to housing policy reforms requires careful modeling of the decision problem faced by prospective homebuyers. The central empirical challenge in analyzing Singapore's Build-to-Order (BTO) allocation system is that raw application rates conflate supply and demand forces. Higher application rates could reflect increased desirability of a project or reduced supply, making naive interpretations misleading for policy evaluation. To address this identification challenge, I develop a discrete choice model grounded in household utility maximization. The key contribution of the model is that changes in application rate post reform reflect changes in the household's valuation of the project.

3.1 Environment

Consider a population of eligible households indexed by i who participate in BTO launch cycles indexed by $t \in \{1, \ldots, T\}$. In each cycle, multiple housing projects $j \in \mathcal{J}_t$ are offered across Singapore's 27 HDB towns. Each project is characterized by observable attributes including location, room type (3-room, 4-room, 5-room), construction wait time and more.

Households must decide whether to submit an application in cycle t and, if so, which single project-room type combination to apply for. This exclusivity constraint—applicants may bid for only one project per cycle—creates a strategic dimension to household decision-making. Crucially, the government sets BTO prices administratively rather than through market clearing, generating persistent excess demand for desirable locations.

3.2 Household Value Functions

I model households as maximizing expected discounted utility from housing. I assume households have perfect information, including of future resale price and probability of success.

A household that applies for project j in cycle t and is successfully allocated receives lifetime utility U_{jt}. Following the dynamic housing literature (Thakral, 2016b; Geyer and Sieg, 2013), I decompose this utility into flow benefits from occupancy and terminal value from eventual resale.

Let MOP_{jt} denote the Minimum Occupancy Period for project j—the mandatory duration before resale is permitted. Under the pre-reform regime, MOP = 5 years for all projects. The November 2021 Prime reform introduced MOP = 10 years for designated prime locations, alongside subsidy clawback provisions and rental restrictions.

The present discounted value of winning project j in cycle t is:

$$V(\text{win})_{jt} = \beta^{B_{jt}} \cdot U_{jt} \tag{1}$$

where $\beta \in (0,1)$ is the annual discount factor and B_{jt} is construction time (typically 3-5 years). The utility term U_{jt} aggregates flow benefits and resale profits:

$$U_{jt} = u_{jt} \cdot \text{MOP}_{jt} + [\pi - \delta_{jt}] \cdot \phi^{\text{MOP}_{jt}} \tag{2}$$

The first term captures flow utility u_{jt} accumulated over the occupancy period. The second term represents expected resale profits: π is the pre-reform profit margin; δ_{jt} captures the effective penalty imposed by the reform; and ϕ^{MOP} discounts future profits back to the present.

For standard (non-Prime) locations, $\delta_{jt} = 0$ both before and after the reform. For Prime locations post-November 2021, $\delta_{jt} > 0$ reflects the combined effect of the 6% subsidy clawback, rental prohibition, and the implicit cost of the extended 10-year MOP.

3.3 Application Decision and Equilibrium

Given the lottery allocation mechanism, a household's expected utility from applying to project j depends on the probability of success P_{jt}:

$$Q(\text{bid})_{jt} = P_{jt} \cdot V(\text{win})_{jt} = P_{jt} \cdot \beta^{B_{jt}} \cdot U_{jt} \tag{3}$$

The success probability is determined by competition. Let N_{jt} denote total applications and S_{jt} denote the supply of units (quota for first-time applicants). Then:

$$P_{jt} = \min\left\{1, \frac{S_{jt}}{N_{jt}}\right\} \tag{4}$$

3.3.1 Indifference Condition

In equilibrium, rational households allocate across projects such that no systematic arbitrage opportunities exist. This implies an indifference condition: the expected value of applying to any project that receives positive applications must be equalized.

Assumption 1 (No-Arbitrage Equilibrium)**.** For all projects $j, j' \in \mathcal{J}_t$ with positive application rates:

$$Q(\text{bid})_{jt} = Q(\text{bid})_{j't} = \bar{Q}(\text{bid})_t \tag{5}$$

This condition constitutes a mixed-strategy Nash equilibrium in the application game. If any project offered strictly higher expected value, households would redirect applications until increased competition restored equality. The equilibrium is stabilized by the self-correcting mechanism: excess applications reduce success probability, which reduces expected value.

3.4 Recovering the Reform Effect

The indifference condition provides the foundation for identifying the reform's impact on the difference in household valuations for prime and non prime units. Define prime towns $\mathcal{J}$ as those designated Prime at least once after November 2021. $\mathcal{K}$ are non-prime towns.

Let τ denote November 2021. For any pre-reform period $n < \tau$ and post-reform period $m \geq \tau$, the equilibrium condition implies:

$$V(win)_{jn} P_{jn} = V(win)_{kn} P_{kn} \quad \forall j \in \mathcal{J}, k \in \mathcal{K} \tag{6}$$

Taking logarithms and averaging across towns and periods:

$$\ln \bar{V}_{j\in\mathcal{J},t<\tau} - \ln \bar{V}_{k\in\mathcal{K},t<\tau} = \ln(\bar{P}_j) - \ln(\bar{P}_k)\Big|_{t<\tau} \tag{7}$$

The analogous expression holds post-reform. Differencing yields the estimating equation for changes in the household valuation of Prime vs Non-Prime properties post reform, θ_{DiD}:

$$\begin{aligned}\theta_{DiD} &= \left[\ln \bar{V}_{j\in\mathcal{J},t\geq\tau} - \ln \bar{V}_{k\in\mathcal{K},t\geq\tau}\right] - \left[\ln \bar{V}_{j\in\mathcal{J},t<\tau} - \ln \bar{V}_{k\in\mathcal{K},t<\tau}\right] \\ &= \left[\ln \bar{P}_j - \ln \bar{P}_k\right]_{t\geq\tau} - \left[\ln \bar{P}_j - \ln \bar{P}_k\right]_{t<\tau}\end{aligned} \tag{8}$$

The reform primarily affects household valuations through parameter δ. Assuming household characteristics for prime and not prime groups remain the same before and after reform, variation in θ is driven primarily by parameter δ, the implicit discount on future resale profits. **Thus, through a DiD estimator we capture the treatment effect on valuation, θ_{DiD}, and indirectly the expected reduction in future resale profits, δ.**

3.5 Failure of Conventional DiD and need for CF-DiD

Conventionally, we would use a difference-in-difference (DiD) study to estimate θ_{DID}. However, due to the failure of parallel trends tests using this method, a machine learning aided DiD was proposed.

To assess the validity of the parallel trends assumption required for standard Difference-in-Differences (DiD), we estimated an event study. We define the treatment group as towns ever designated "Prime" and the control group as those that were not. We estimated the dynamic specification $y_{it} = \alpha_i + \gamma_t + \sum_{k\neq -1} \beta_k \cdot (\text{EverPrime}_i \times \mathbf{1}_{t=k}) + \epsilon_{it}$, including town and period fixed effects with standard errors clustered at the town level. The results, presented in Figure 1, strongly reject the null hypothesis of parallel trends. The pre-treatment coefficients exhibit substantial volatility, ranging from 0.2 to 1.8, with confidence intervals that exclude zero in 10 of the pre-treatment periods. A joint Wald test on the pre-treatment coefficients yields a p-value of 0.00, confirming systematic differential trends between Prime and Standard locations prior to the reform.

This violation of unconditional parallel trends is likely driven by significant compositional differences between the groups and the sparsity of the treatment data (50 treated vs. 367 control observations in the pre-period). Prime locations systematically differ in observable characteristics—such as proximity to the CBD and amenities—which likely generate divergent bidding dynamics independent of the policy. To address this identification challenge, we adopt a Causal Forest Difference-in-Differences (CF-DiD) framework (Gavrilova et al., 2025). This approach allows us to relax the strict unconditional parallel trends assumption in favor of *conditional* parallel trends. By leveraging high-dimensional controls to adjust for these confounding observables, CF-DiD provides a more credible identification strategy in the presence of such structural imbalances.

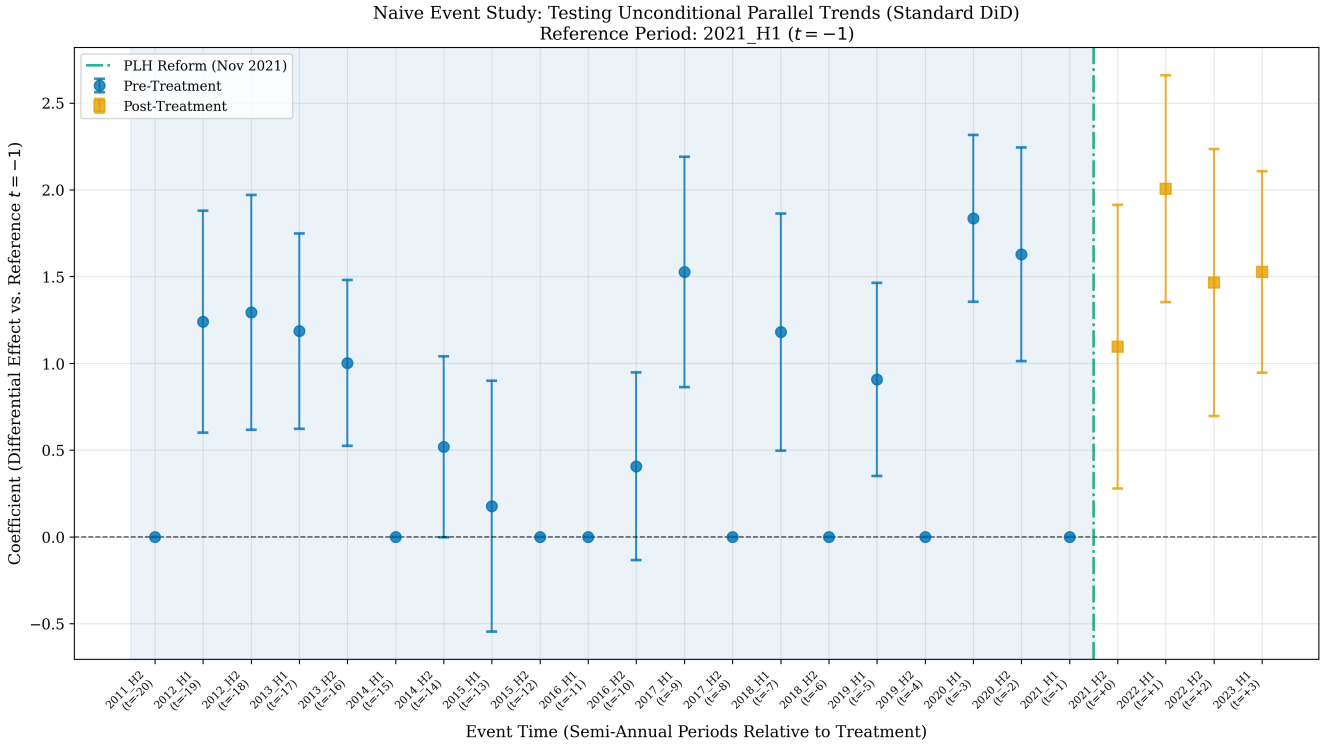

Figure 1. **Naive Event Study: Testing Unconditional Parallel Trends.** This figure displays coefficients from a standard difference-in-differences event study: $Y_{it} = \alpha_{\text{town}} + \gamma_{\text{period}} + \sum_{k \neq -1} \beta_k(\text{EverPrime}_i \times \mathbf{1}[\text{period} = k]) + \epsilon_{it}$. Semi-annual periods; reference period is 2021_H1 ($t = -1$). Standard errors clustered at town level. Blue circles = pre-treatment; orange squares = post-treatment. Error bars show 95% CIs. *Interpretation:* Pre-treatment coefficients range from 0.2 to 1.8 with many CIs excluding zero. Multiple pre-periods show significant differential effects (e.g., $\beta_{-3} = 1.84$, $\beta_{-2} = 1.63$). Joint F-test rejects parallel trends ($p < 0.001$). *Implication:* Unconditional parallel trends is **violated**. Prime and Non-Prime locations exhibit systematically different outcome trajectories, motivating the CF-DiD approach that conditions on observables to restore identification.

4 Causal Forest Difference-in-Differences

This section introduces the Causal Forest Difference-in-Differences (CF-DiD) framework used to estimate the treatment effect $\hat{\theta}$ derived in Section 3. Section 4.1 describes the CF-DiD methodology and its identifying assumptions. Section 4.2 demonstrates how CF-DiD maps to the economic model and justifies its appropriateness for this setting.

4.1 Causal Forest DiD Methodology

Developed by Wager and Athey (2018) and generalised by Athey et al. (2019), causal forests are a machine learning method for estimating heterogeneous treatment effects, extending the random forest algorithm to causal inference settings. A standard random forest constructs an ensemble of decision trees, each trained on a bootstrap sample of the data, with predictions averaged across trees to reduce variance. Causal forests adapt this framework by modifying the tree-splitting criterion: rather than minimizing prediction error, splits are chosen to maximize heterogeneity in treatment effects across the resulting subgroups. This produces a flexible, nonparametric estimator that can capture complex interactions between covariates and treatment effects without requiring the researcher to specify functional forms.

Gavrilova et al. (2025) extends the Causal Forest estimator to difference-in-differences settings. In the context of difference-in-differences, the causal forest learns the conditional expectation of outcomes given covariates among control units, enabling construction of unit-specific counterfactuals. By training on the control group across all time periods, the forest captures how observable characteristics predict outcome trajectories absent treatment. For treated units in the post-period, the trained model imputes what their outcomes would have been under the control condition, and treatment effects are recovered as the difference between observed and predicted values.

Gavrilova et al. (2025) key innovation is relaxing the unconditional parallel trends assumption of Athey et al. (2019) in favor of *conditional* parallel trends, which permits consistent estimation when treated and control units differ systematically in observable characteristics. See appendix C for a more detailed history of machine learning augmented DiD approaches.

4.1.1 Setup and Notation

Consider a panel of units $i \in \{1, \ldots, N\}$ observed over periods $t \in \{1, \ldots, T\}$, with treatment occurring at time τ. Let $D_i \in \{0, 1\}$ denote time-invariant treatment assignment, $\text{Post}_t = \mathbf{1}[t \geq \tau]$ the post-treatment indicator, and Y_{it} the observed outcome. Under the potential outcomes framework, $Y_{it}(0)$ and $Y_{it}(1)$ denote outcomes under control and treatment, respectively. The observed outcome satisfies:

$$Y_{it} = Y_{it}(0) + D_i \cdot \text{Post}_t \cdot [Y_{it}(1) - Y_{it}(0)] \tag{9}$$

The estimand of interest is the Average Treatment Effect on the Treated (ATT):

$$\theta_{\text{ATT}} = \mathbb{E}\left[Y_{it}(1) - Y_{it}(0) \mid D_i = 1, t \geq \tau\right] \tag{10}$$

4.1.2 Identifying Assumption: Conditional Parallel Trends

Standard DiD requires the unconditional parallel trends assumption:

$$\mathbb{E}\left[\Delta Y_{it}(0) \mid D_i = 1\right] = \mathbb{E}\left[\Delta Y_{it}(0) \mid D_i = 0\right] \tag{11}$$

which states that absent treatment, treated and control units would have evolved identically on average. As demonstrated in Section 3.5, this assumption fails in the present context due to systematic compositional differences between Prime and non-Prime locations.

CF-DiD instead requires the weaker *conditional* parallel trends assumption:

Assumption 2 (Conditional Parallel Trends)**.** For all x in the support of X:

$$\mathbb{E}\left[\Delta Y_{it}(0) \mid D_i = 1, X_i = x\right] = \mathbb{E}\left[\Delta Y_{it}(0) \mid D_i = 0, X_i = x\right] \tag{12}$$

This assumption states that conditional on observables X_i, treated and control units would have followed parallel paths absent treatment. The assumption is plausible when selection into treatment depends on observables that also affect outcome trajectories—precisely the case for Prime location designation, which correlates with proximity to the CBD, amenities, and other location characteristics that independently influence bidding dynamics.

4.1.3 Estimation Procedure

The CF-DiD estimator proceeds in four steps, following Gavrilova et al. (2025):

Step 1: Outcome Model Estimation. Train a flexible outcome model $\hat{\mu}(X_i, t)$ on control group observations ($D_i = 0$) across all time periods. This model captures the conditional expectation $\mathbb{E}[Y_{it} \mid X_{i,t}, D_i = 0]$. Following Athey et al. (2019), we employ a random forest regressor to accommodate potentially complex, nonlinear relationships between covariates and outcomes.

Step 2: Counterfactual Prediction. For each treated unit i with $D_i = 1$ in the post-treatment period ($t \geq \tau$), predict the counterfactual outcome:

$$\hat{Y}_{it}(0) = \hat{\mu}(X_i, t) \tag{13}$$

This imputes what the outcome would have been absent treatment, conditional on the unit's characteristics and the time period.

Step 3: Individual Treatment Effect Computation. Compute individual treatment effects for treated units in the post-period:

$$\hat{\tau}_i = Y_{it} - \hat{Y}_{it}(0) \tag{14}$$

Step 4: ATT Estimation. The ATT is estimated as the average of individual effects:

$$\hat{\theta}_{\text{CF-DiD}} = \frac{1}{N_1^{\text{post}}} \sum_{i: D_i = 1, t \geq \tau} \hat{\tau}_i \tag{15}$$

where N_1^{post} denotes the number of treated observations in the post-period.

4.1.4 Inference via Clustered Bootstrap

Standard errors are computed via clustered bootstrap at the panel unit level to account for within-unit serial correlation (Cameron and Miller, 2015). For each bootstrap iteration $b \in \{1, \ldots, B\}$:

1. Resample panel units with replacement
2. Re-estimate the outcome model on control observations

3. Recompute counterfactuals and treatment effects

4. Calculate bootstrap ATT: $\hat{\theta}^{(b)}$

The standard error is $\widehat{\text{SE}} = \sqrt{\text{Var}(\hat{\theta}^{(b)})}$, and confidence intervals are constructed using bootstrap percentiles.

4.1.5 Additional Assumptions

Beyond conditional parallel trends, identification requires:

Assumption 3 (Overlap)**.** For all x in the support of X: $0 < \Pr(D_i = 1 \mid X_i = x) < 1$.

This ensures sufficient overlap in covariate distributions between treated and control groups, enabling counterfactual extrapolation. Given that Prime locations constitute a subset of the covariate space (central, high-amenity areas), this assumption requires control units with similar characteristics—a condition supported by the presence of a few centrally-located high-amenity non-Prime towns in our data. See figure A2 for the distribution of distance to key amenities by Prime Location Status.

Assumption 4 (No Anticipation)**.** $Y_{it}(1) = Y_{it}(0)$ for all $t < \tau$.

This rules out anticipatory behavioral responses prior to the November 2021 reform. The assumption is reasonable given that the PLH policy was announced shortly before implementation, limiting opportunities for strategic pre-adjustment. This is tested in table 3.

4.1.6 Validation: Placebo Tests

We validate conditional parallel trends via placebo tests. For candidate placebo dates $\tilde{\tau} < \tau$ in the pre-treatment period, we estimate pseudo-treatment effects. Under the null of valid identification, placebo effects should be statistically indistinguishable from zero. Systematic non-zero placebo effects would indicate pre-existing differential trends that bias the true treatment effect estimate.

4.2 Application to the PLH Reform

The CF-DiD framework maps directly to the theoretical model in Section 3. Recall that the estimand of interest is the change in household valuations of Prime versus non-Prime locations following the reform:

$$\theta_{\text{DiD}} = \left(\ln \bar{P}_j - \ln \bar{P}_k\right)_{t \geq \tau} - \left(\ln \bar{P}_j - \ln \bar{P}_k\right)_{t < \tau} \tag{16}$$

where P_{jt} denotes first-timer success probability. In the CF-DiD implementation:

- **Outcome**: $Y_{it} = \ln P_{it}^{\text{first}}$, the log probability of first-timer allocation for town-room combination i in cycle t
- **Treatment**: $D_i = \mathbf{1}[\text{EverPrime}_i]$, indicating locations designated Prime at any point post-reform
- **Post-period**: $\text{Post}_t = \mathbf{1}[t \geq \text{November 2021}]$
- **Covariates**: X_i includes location attributes (distance to CBD, MRT, parks, schools), project characteristics (room type, construction wait time), and macroeconomic conditions

The CF-DiD estimator $\hat{\theta}_{\text{CF-DiD}}$ thus provides a consistent estimate of θ_{DiD} under Assumptions 2–4. Through the equilibrium relationship derived in Equation (8), this identifies the reform's impact on household valuations and, indirectly, the implicit discount δ on future resale profits imposed by the PLH restrictions.

The approach is particularly well-suited to this context for three reasons. First, Prime locations differ systematically from control locations in observables correlated with bidding dynamics, violating unconditional parallel trends but plausibly satisfying conditional parallel trends. Second, the high-dimensional covariate space (21 features after VIF selection) benefits from the random forest's ability to capture complex interactions without parametric specification. Third, the small treated sample ($N = 23$ post-treatment observations) necessitates efficient use of control group information for counterfactual imputation, which the outcome-modeling approach provides.

5 Data and Empirical Implementation

This section describes the dataset construction (Section 5.1), the estimation procedure (Section 5.2), and inference methods appropriate for small-sample settings (Section 5.3).

5.1 Dataset

The analysis draws on a novel panel dataset of BTO launch outcomes constructed from multiple administrative sources. The dataset comprises 493 observations spanning 73 unique town-room combinations (panel units) from November 2011 to August 2023, the analysis window selected to isolate the PLH reform from subsequent policy changes.[1]

5.1.1 Data Sources and Construction

The dataset integrates four categories of variables:

(i) BTO Launch Outcomes. Application counts, unit supply, and allocation outcomes by applicant type (first-timer, second-timer) were obtained from the Housing Development Board's public launch records.[2] The primary outcome variable is:

$$\ln P_{it}^{\text{first}} = \ln \left(\min \left\{ 1, \frac{S_{it}^{\text{first}}}{N_{it}^{\text{first}}} \right\} \right) \tag{17}$$

where S_{it}^{first} and N_{it}^{first} denote the first-timer quota and application count, respectively.

(ii) Project-Specific Features. Location attributes include Geodesic distances (in km) to: the Central Business District (MBFC), nearest MRT station, parks, supermarkets, hawker centers, shopping malls, elite primary schools, and existing HDB developments. Construction characteristics include room type (3-room, 4-room, 5-room) and expected wait time.

(iii) Macroeconomic Indicators. Time-varying controls include the Consumer Price Index (CPI), Straits Times Index (STI) closing price and volume, per capita GNI, and the average monthly Singapore Overnight Rate Average (SORA).

(iv) Cycle Characteristics. Variables capturing the competitive environment within each launch cycle, including total supply and median distance to CBD across all projects offered.

[1] The August 2023 cutoff precedes the introduction of rejection penalties that altered the strategic environment.

[2] Application rates data were purchased from Teoalida, who maintains a record of the HDB public launch site.

5.1.2 Treatment and Control Groups

The treatment indicator EverPrime_i equals one for town-room combinations located in areas designated Prime Location Housing at any point after November 2021. This intent-to-treat definition captures the policy's effects on locations subject to the new regime, regardless of the specific launch timing.

Table 1 reports summary statistics by treatment status. The analysis sample contains 76 post-policy observations (23 treated, 53 control) and 417 pre-policy observations (50 treated, 367 control). Prime locations exhibit systematically lower mean distances to CBD (3.2 km vs. 8.7 km) and higher application rates pre-reform, motivating the conditional parallel trends approach.

Table 1. Summary Statistics by Treatment Status and Period

	Pre-Reform		Post-Reform	
	Control	Treated	Control	Treated
$\ln P^{\text{first}}$	-0.663	-1.090	-1.090	-0.863
	(0.657)	(0.814)	(0.825)	(0.746)
Distance to CBD (km)	14.227	6.789	14.657	4.921
	(3.265)	(2.415)	(3.347)	(2.146)
Distance to MRT (km)	0.717	0.555	0.983	0.327
	(0.491)	(0.325)	(0.630)	(0.224)
Wait Time (months)	45.422	55.080	51.679	66.261
	(7.123)	(7.292)	(10.370)	(6.390)
N	367	50	53	23

Notes: Summary statistics for key variables by treatment status (EverPrime = 1 for locations designated Prime post-reform) and period (Pre-Reform: before November 2021; Post-Reform: November 2021–August 2023). Means with standard deviations in parentheses. $\ln P^{\text{first}}$ is the log probability of first-timer allocation. Distance to CBD measured to Marina Bay Financial Centre. Treated locations are systematically closer to CBD (6.8 vs 14.2 km), motivating the conditional parallel trends approach.

5.1.3 Feature Selection via VIF Analysis

To address multicollinearity among the 23 candidate covariates, we employ iterative Variance Inflation Factor (VIF) analysis with a threshold of 5.0 (O'Brien, 2007). This procedure removed two highly collinear variables (per capita GDP, VIF = 147.2; CPI, VIF = 9.7), yielding 21 retained features with VIF < 5.

5.2 Estimation Procedure

The CF-DiD model is estimated following the procedure in Section 4.1:

Outcome Model Specification. The random forest regressor is trained on control group observations (EverPrime = 0) with the following hyperparameters: 500 trees, minimum leaf size of 5 observations, and no maximum depth restriction. Time fixed effects are incorporated via period dummy variables appended to the feature matrix, allowing flexible time trends.

Feature Set. The 21 covariates retained after VIF selection include:

- *Distance measures* (10): CBD, MRT, park, supermarket, hawker center, road, existing HDB, under-construction HDB, mall, elite school
- *Location*: Longitude
- *Project characteristics* (2): Room number, wait time
- *Macroeconomic* (4): STI close, STI volume, per capita GNI, SORA
- *Cycle characteristics* (4): Current/next cycle supply, current/next cycle median CBD distance

Full feature importance analysis for the random forest model is available in appendix C.

Counterfactual Prediction. For each of the 23 treated post-reform observations, we predict the counterfactual outcome using the trained model and compute individual treatment effects as the difference between observed and predicted values.

5.3 Inference for Small Samples

The small treated post-reform sample ($N = 23$) poses challenges for standard asymptotic inference. We address this through:

Clustered Bootstrap. Standard errors are computed via 200 bootstrap replications, resampling at the panel unit level to preserve within-unit correlation structure. This approach provides valid inference under cluster dependence (Cameron and Miller, 2015).

Percentile Confidence Intervals. The 95% confidence interval is constructed as $[\hat{\theta}_{0.025}, \hat{\theta}_{0.975}]$, where $\hat{\theta}_\alpha$ denotes the α-quantile of the bootstrap distribution. This avoids normal approximations that may perform poorly in small samples.

Robustness via Placebo Tests. Rather than relying solely on point estimates and standard errors, we assess identification validity through placebo tests at 8 randomly selected pre-treatment dates. Under valid identification, placebo effects should cluster around zero.

6 Results and Discussion

This section presents the main empirical findings. Section 6.1 reports the CF-DiD treatment effect estimate. Section 6.2 presents validation tests for the parallel trends assumption. Section 6.3 examines the dynamic treatment effect pattern.

6.1 Main Results: Treatment Effect Estimate

Table 2 reports the CF-DiD estimation results. The estimated ATT is 0.500 (SE = 0.229), statistically significant at the 5% level ($p = 0.029$). The 95% bootstrap confidence interval of $[0.183, 1.005]$ excludes zero, providing evidence of a positive treatment effect.

6.1.1 Interpretation

The positive ATT estimate requires careful interpretation in light of the theoretical model. The outcome variable is $\ln P^{\text{first}}$, the log probability of first-timer success. The equilibrium condition (Equation 5) implies:

$$\ln P_{jt} = \ln \bar{Q}_t - \ln V_{jt}^{\text{win}} \tag{18}$$

Table 2. DID-CF Estimation Results: Effect of Prime Location Policy on First-Timer Allocation Probability

Panel A: Main Results	
ATT Estimate	0.5002
	(0.2290)
t-statistic	2.18
p-value	0.029
95% Confidence Interval	[0.183, 1.005]
Panel B: Parallel Trends Test	
Treatment × Time Coefficient	−0.306
	(0.345)
p-value	0.376
Panel C: Placebo Tests	
Number of Placebo Tests	8
Significant Placebo Effects	0
Mean Placebo Effect	−0.094

Notes: Panel A reports the Average Treatment Effect on the Treated (ATT) from the CF-DiD model. Standard errors (in parentheses) computed via clustered bootstrap at the town-room level with 200 replications. Panel B reports the coefficient on Treatment × Time from a pre-treatment regression testing for differential trends. Panel C summarizes placebo tests at 8 randomly selected pre-treatment dates; significance defined as 95% CI excluding zero.

A higher $\ln P_{jt}$ thus corresponds to *lower* household valuation V_{jt}^{win}, holding the reservation utility $\bar{Q}_t$ constant. The positive ATT of 0.50 indicates that Prime locations experienced a 0.50 log-point increase in first-timer success probability relative to the control group counterfactual—equivalently, a *decrease* in household valuation of approximately 50 log points, or roughly 65% in level terms ($e^{0.50} - 1 \approx 0.65$).

This finding is consistent with the theoretical prediction that PLH restrictions reduce demand for affected properties by diminishing expected resale profits. Through the lens of the model, the result implies a substantial implicit discount $\delta > 0$ on future windfall gains, reflecting the combined deterrent effect of the extended MOP, rental prohibition, subsidy clawback, and resale buyer restrictions.

6.1.2 Magnitude Assessment

The estimated effect size is economically meaningful. A 0.50 increase in log success probability corresponds roughly to a halving of the application-to-supply ratio. For a project with a pre-reform oversubscription rate of 10:1 (success probability 10%), the implied post-reform rate would be approximately 6:1 (success probability 16.5%). This demand reduction is substantial given the policy's intent to dampen speculative bidding on prime locations.

6.2 Validation of Identifying Assumptions

The validity of the CF-DiD estimate depends on the conditional parallel trends assumption. We assess this through two complementary approaches.

6.2.1 Pre-Treatment Parallel Trend Test

We test for differential pre-treatment trends using the specification:

$$Y_{it} = \alpha_i + \beta t + \gamma(D_i \times t) + \epsilon_{it}, \quad t < \tau \tag{19}$$

where α_i are panel fixed effects and t is a normalized time trend. Under parallel trends, $\gamma = 0$. The null hypothesis is tested via a t-statistic with standard errors clustered at the panel level:

$$t_\gamma = \frac{\hat{\gamma}}{\widehat{\text{SE}}(\hat{\gamma})} \tag{20}$$

Panel B of Table 2 reports results from a regression of outcomes on treatment status interacted with a linear time trend, estimated on pre-treatment data with panel fixed effects. The coefficient on Treatment × Time is -0.306 (SE $= 0.345$, $p = 0.376$), statistically indistinguishable from zero. This provides no evidence against parallel pre-trends conditional on fixed effects.

Importantly, this test differs from the unconditional event study in Figure **??**, which rejected parallel trends. The CF-DiD framework conditions on a richer set of covariates, allowing for parallel trends to hold conditionally even when they fail unconditionally.

6.2.2 Placebo Tests

For candidate placebo dates $\tilde{\tau} < \tau$ in the pre-treatment period, we estimate pseudo-treatment effects:

$$\hat{\theta}^{\text{placebo}}(\tilde{\tau}) = \frac{1}{N_1^{\tilde{\tau}}} \sum_{i:D_i=1, t \geq \tilde{\tau}}^{t<\tau} \left(Y_{it} - \hat{\mu}^{(\tilde{\tau})}(X_i, t) \right) \tag{21}$$

where $\hat{\mu}^{(\tilde{\tau})}(X_i, t)$ is the counterfactual prediction from a model treating $\tilde{\tau}$ as the policy date. Under valid identification, $\mathbb{E}[\hat{\theta}^{\text{placebo}}(\tilde{\tau})] = 0$ for all $\tilde{\tau} < \tau$.

Panel C of Table 2 and Figure 2 reports placebo test results. We estimate pseudo-treatment effects at 8 randomly selected pre-treatment dates using the full CF-DiD procedure. Key findings:

- Zero of 8 placebo effects are statistically significant (95% CI excluding zero)
- Mean placebo effect is -0.094, close to the theoretical null of zero
- Standard deviation of placebo effects is 0.036, substantially smaller than the true effect (0.500)

The clustering of placebo effects around zero, combined with the distinctly larger true treatment effect, supports the validity of the identification strategy. If systematic pre-trends contaminated the estimate, we would expect non-zero placebo effects of similar magnitude to the true effect.

6.2.3 Anticipation Effects Test

Finally we test the no anticipation assumption in table 3. As expected, the coefficient is insignificant, implying adherence to the assumption and supporting validity of CF-DiD.

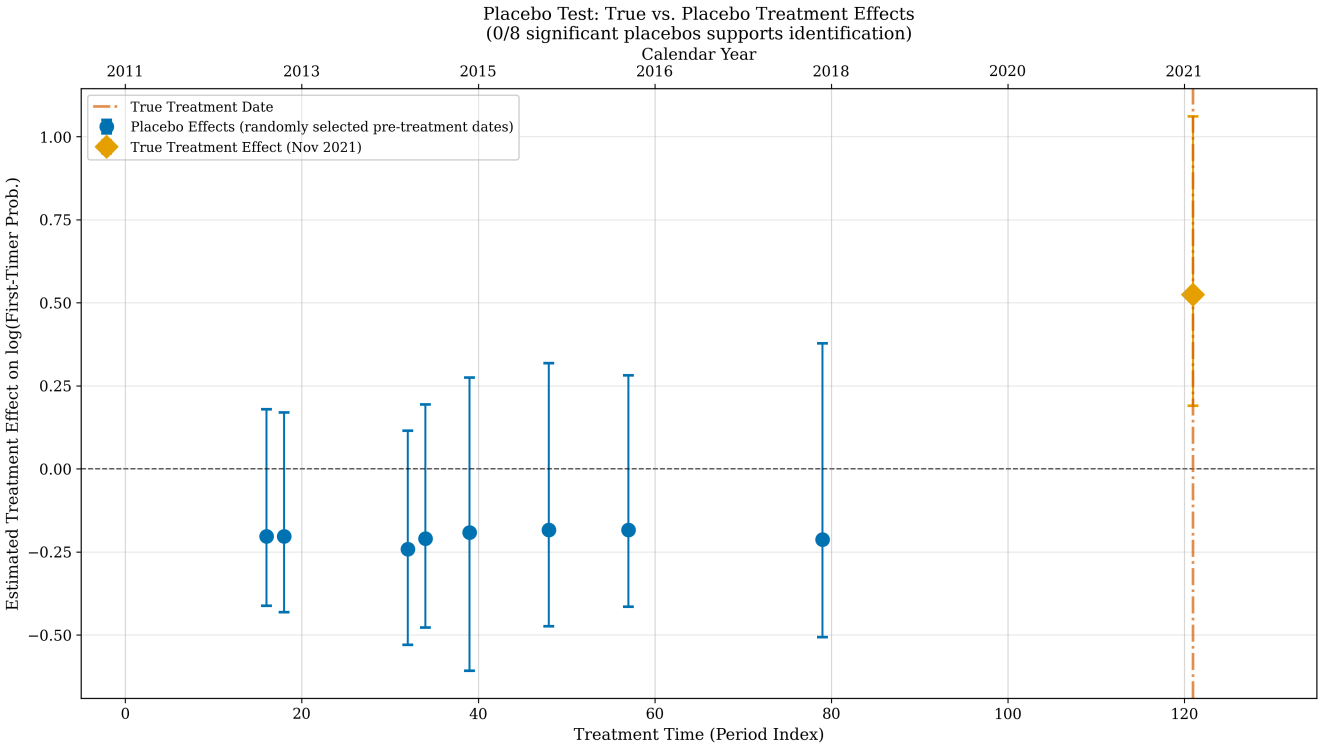

Figure 2. **Placebo Test: Validation of Identification Strategy.** This figure compares the estimated CF-DiD treatment effect at the true policy date (November 2021, orange diamond, ATT = 0.52) against placebo effects at 8 randomly selected pre-treatment dates (blue circles). Placebo dates drawn from periods at least 6 months before treatment to avoid announcement effects: March 2013, May 2013, July 2014, September 2014, February 2015, November 2015, August 2016, June 2018. Error bars show 95% bootstrap CIs. Bottom axis: period index; top axis: calendar years. *Interpretation:* (1) All 8 placebo CIs cross zero (0/8 significant at 5% level); (2) Mean placebo effect is −0.20, near zero and distinctly different from true effect of +0.52; (3) SD of placebo effects is 0.02, indicating low noise in the pre-period. *Implication:* The absence of spurious pre-treatment effects strongly supports the CF-DiD identification strategy. The true effect reflects policy impact rather than pre-existing trends.

Table 3. Test for Anticipation Effects

	Coefficient	Std. Error
Anticipation Effect (δ)	-0.2171	(0.4340)
t-statistic	-0.500	
p-value	0.6169	
Post-Treatment Effect (θ)	0.4502	(0.1424)
t-statistic	3.161	
p-value	0.0016	
Panel FE	Yes	
Time FE	Yes	
Observations	493	

Notes: Test for anticipation effects using specification: $Y_{it} = \alpha_i + \gamma_t + \delta(D_i \times \mathbf{1}[t \in [\tau - 6, \tau)]) + \theta(D_i \times \mathbf{1}[t \geq \tau]) + \epsilon_{it}$. Anticipation window: Jun 2021–Nov 2021 (6 months before reform). Standard errors clustered at town-room level. The insignificant anticipation coefficient ($p = 0.617$) supports the no-anticipation assumption.

6.3 Event Study: Dynamic Treatment Effects

I estimate an event study to analyse dynamic treatment effects across periods. The event study estimates period-specific treatment effects releative to the policy date:

$$\hat{\tau}_e = \frac{1}{N_e} \sum_{i:D_i=1, t-\tau=e} (Y_{it} - \hat{\mu}(X_i, t)) \tag{22}$$

where $e = t - \tau$ denotes event time (periods relative to policy implementation), $\hat{\mu}(X_i, t)$ is the random forest counterfactual prediction trained on control observations, and N_e is the number of treated observations in event period e. Under conditional parallel trends, $\mathbb{E}[\hat{\tau}_e] = 0$ for $e < 0$ (pre-treatment periods) and $\mathbb{E}[\hat{\tau}_e] = \tau_e$ for $e \geq 0$ (post-treatment periods).

Figure 3 presents the event study. Several patterns emerge:

Pre-Treatment Period. Coefficients fluctuate around zero without systematic trend. While some individual periods show marginally significant effects (reflecting sampling variation with sparse treatment observations), there is no discernible pattern of differential pre-trends. This visual evidence complements the formal parallel trends test.

Post-Treatment Dynamics. Treatment effects exhibit a positive and increasing trajectory after November 2021. Initial effects (periods 0–6) are positive but imprecisely estimated, with confidence intervals spanning zero. Later periods (12–18) show larger, statistically significant effects ranging from 0.62 to 0.94. This pattern suggests the policy's demand-reducing effect strengthened over time as market participants internalized the new regime.

The increasing post-treatment trajectory is consistent with learning dynamics in the housing market. Applicants may have initially underestimated the policy's impact on resale profitability, with demand adjustments accelerating as information diffused and the new equilibrium emerged.

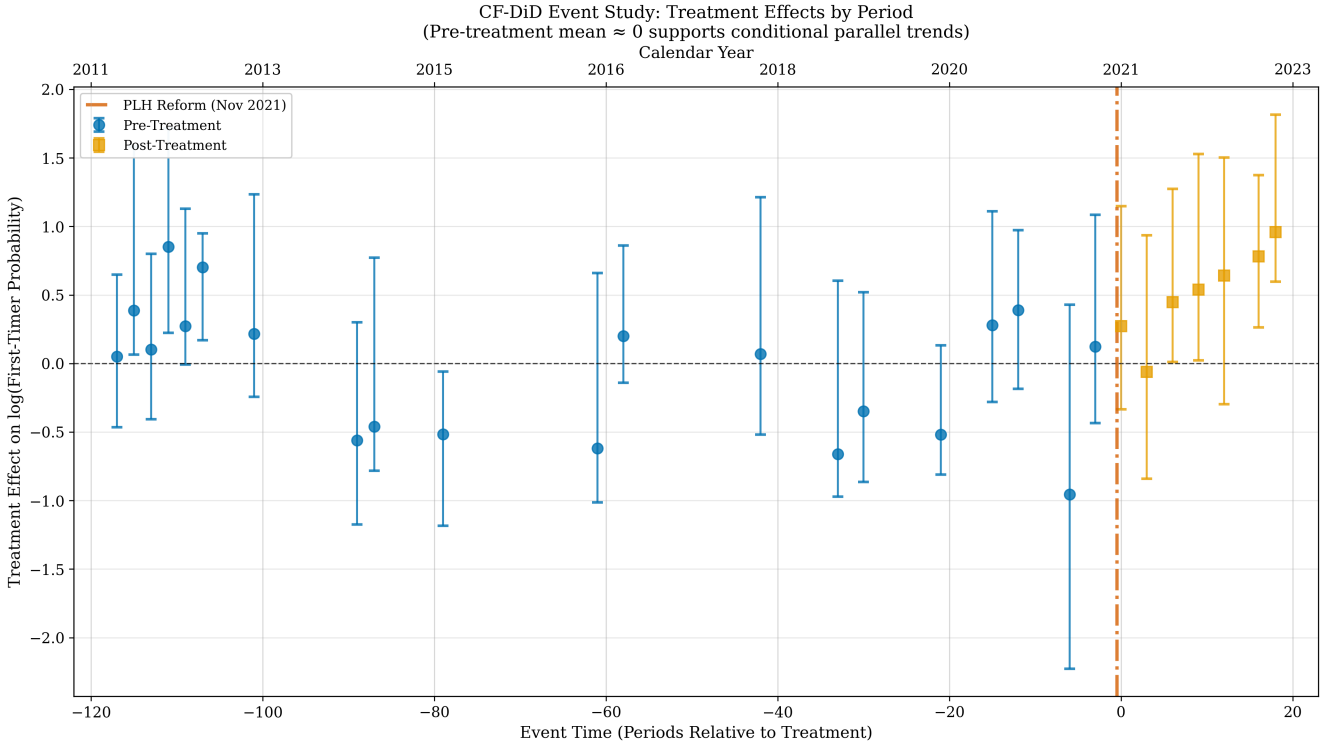

Figure 3. **CF-DiD Event Study: Treatment Effects by Period.** This figure displays period-specific treatment effects from the Causal Forest Difference-in-Differences model following Gavrilova et al. (2025). Each point represents $\hat{\tau}_e = N_e^{-1} \sum_{i:D_i=1, t-\tau=e} (Y_{it} - \hat{\mu}(X_i, t))$, the mean difference between observed outcomes and random forest counterfactual predictions. Blue circles = pre-treatment; orange squares = post-treatment. Error bars show 95% bootstrap CIs (200 replications, clustered at town-room level). Bottom axis: event time (periods relative to Nov 2021); top axis: calendar years. *Interpretation:* (1) Pre-treatment effects have mean ≈ -0.05, close to zero, with most CIs overlapping zero—unlike Figure 1, conditioning on covariates removes differential pre-trends; (2) Post-treatment effects are positive and growing: 0.27 at $t = 0$, 0.45 at $t = 6$, 0.64 at $t = 12$, 0.78 at $t = 16$, 0.96 at $t = 18$. *Implication:* The policy effect emerges at implementation and strengthens over time, consistent with market learning dynamics.

7 Conclusion

This paper provides the first empirical evaluation of Singapore's 2021 Prime Location Housing reform, estimating its effect on BTO demand using a Causal Forest Difference-in-Differences framework.

7.1 Summary of Findings

The main result is a positive and statistically significant ATT of 0.50 log points on first-timer success probability ($p = 0.029$, 95% CI: [0.18, 1.01]). Through the lens of the equilibrium model, this implies a substantial reduction in household valuations for Prime locations post-reform—consistent with the policy's intent to dampen speculative demand by restricting resale profitability.

The identification strategy passes multiple validation tests. Conditional parallel trends cannot be rejected ($p = 0.376$), and placebo tests at 8 pre-treatment dates yield zero significant effects with a mean near zero. The event study reveals treatment effects emerging at implementation and strengthening over subsequent periods, consistent with market learning dynamics.

7.2 Policy Implications

The findings suggest the PLH reform successfully reduced demand for centrally-located public housing. From a policy perspective, this provides evidence that restrictions on housing resale profitability can meaningfully influence allocation patterns—addressing concerns about windfall gains and speculative bidding that motivated the reform.

The estimated demand reduction of approximately 65% (in level terms) is substantial. However, the policy's ultimate welfare implications depend on factors beyond this paper's scope, including: (i) whether reduced demand translates to improved access for genuine owner-occupiers versus reduced overall interest; (ii) distributional effects across income groups; and (iii) long-term consequences for residential mobility and housing market efficiency.

7.3 Limitations

Several limitations warrant acknowledgment:

Small Sample Size. The analysis relies on 23 treated post-reform observations, limiting statistical power and precluding detailed heterogeneity analysis. Bootstrap inference partially addresses this, but results should be interpreted as suggestive rather than definitive.

Short Post-Treatment Window. The analysis period ends August 2023, providing approximately 22 months of post-reform data. The strengthening treatment effects over time suggest full equilibrium adjustment may not yet have occurred.

Conditional Parallel Trends. While placebo tests support the identifying assumption, conditional parallel trends remains untestable in finite samples. Residual confounding from unobserved time-varying factors cannot be fully ruled out.

External Validity. Singapore's unique housing system limits generalizability to other contexts. The findings inform policy design in similarly structured lottery allocation systems but may not extend to market-clearing housing markets.

7.4 Directions for Future Research

This study opens several avenues for future work. First, extending the analysis window as additional post-reform launches occur will improve precision and enable assessment of long-run equilibrium effects. Second, the first PLH units reach resale eligibility in 2031; tracking actual resale outcomes will permit direct estimation of the implicit discount δ rather than inference through demand responses. Third, structural estimation of the discrete choice model could recover preference parameters and enable counterfactual policy simulations. Finally, the CF-DiD methodology developed here may prove useful for evaluating housing policies in other lottery allocation systems worldwide.

In sum, this paper demonstrates that Singapore's Prime Location Housing reform achieved its proximate goal of reducing demand for affected properties. Whether this translates to the reform's ultimate objectives—dampening speculative behavior and ensuring equitable access to centrally-located public housing—remains an important question for continued empirical investigation.

A Descriptive Analysis

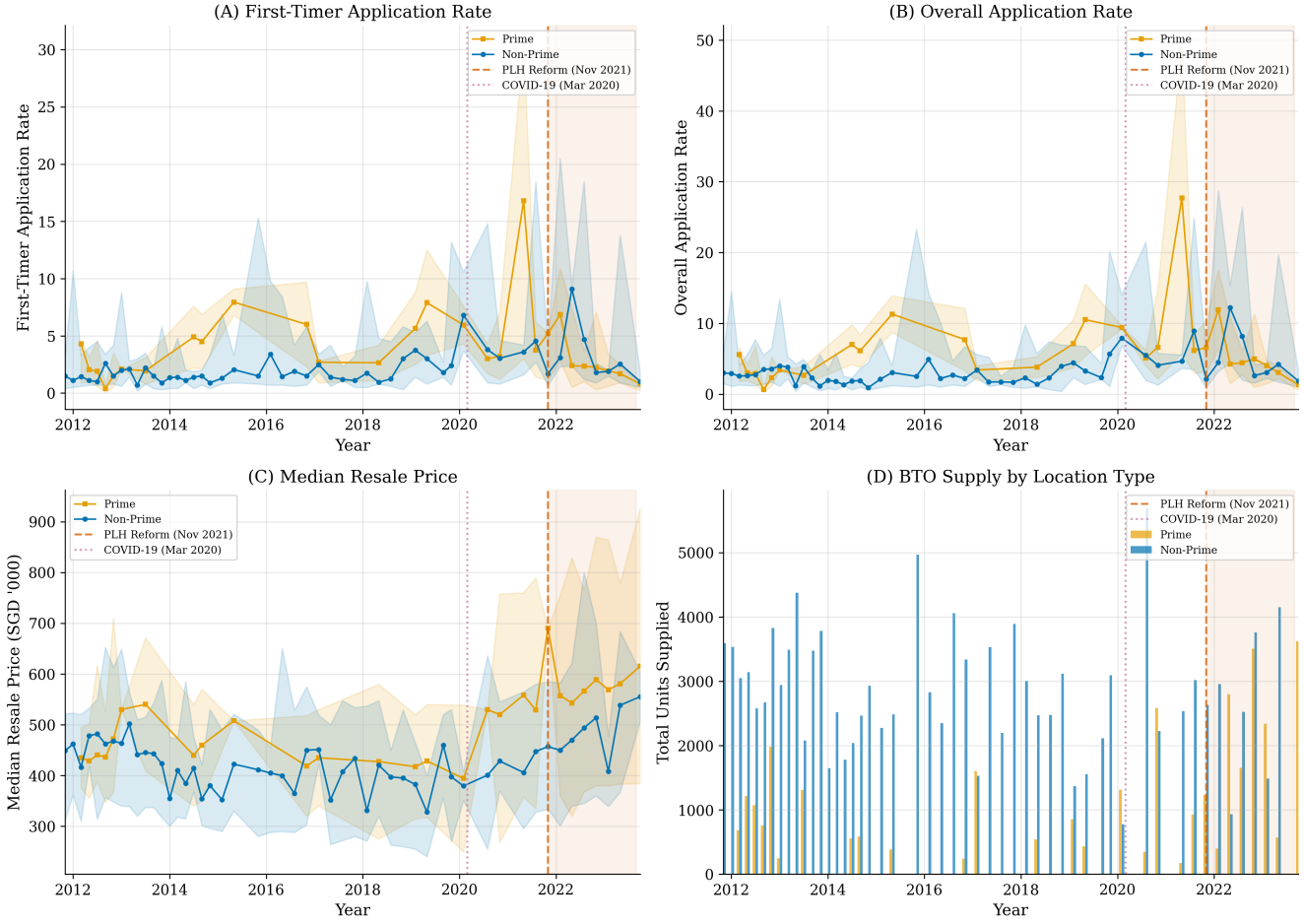

Appendix Figure A1. **Descriptive Time Series by Prime Location Status, 2011–2023.** This figure presents key housing market indicators for Prime (orange squares) and Non-Prime (blue circles) locations. Solid lines show median values; shaded regions indicate the min-max range. The vertical dashed red line marks PLH reform implementation (November 2021); the dotted pink line marks COVID-19 onset (March 2020). *Panel A:* First-timer application rates show Prime locations consistently experience higher oversubscription. Post-reform, Prime rates decline. *Panel B:* Overall application rates exhibit similar patterns. *Panel C:* Median resale prices diverge over time, with Prime locations commanding a premium that widened during 2020–2022. *Panel D:* BTO supply by location type shows the relative scale of Prime vs Non-Prime launches. *Implication:* Visual evidence suggests the PLH reform coincided with reduced demand for Prime locations.

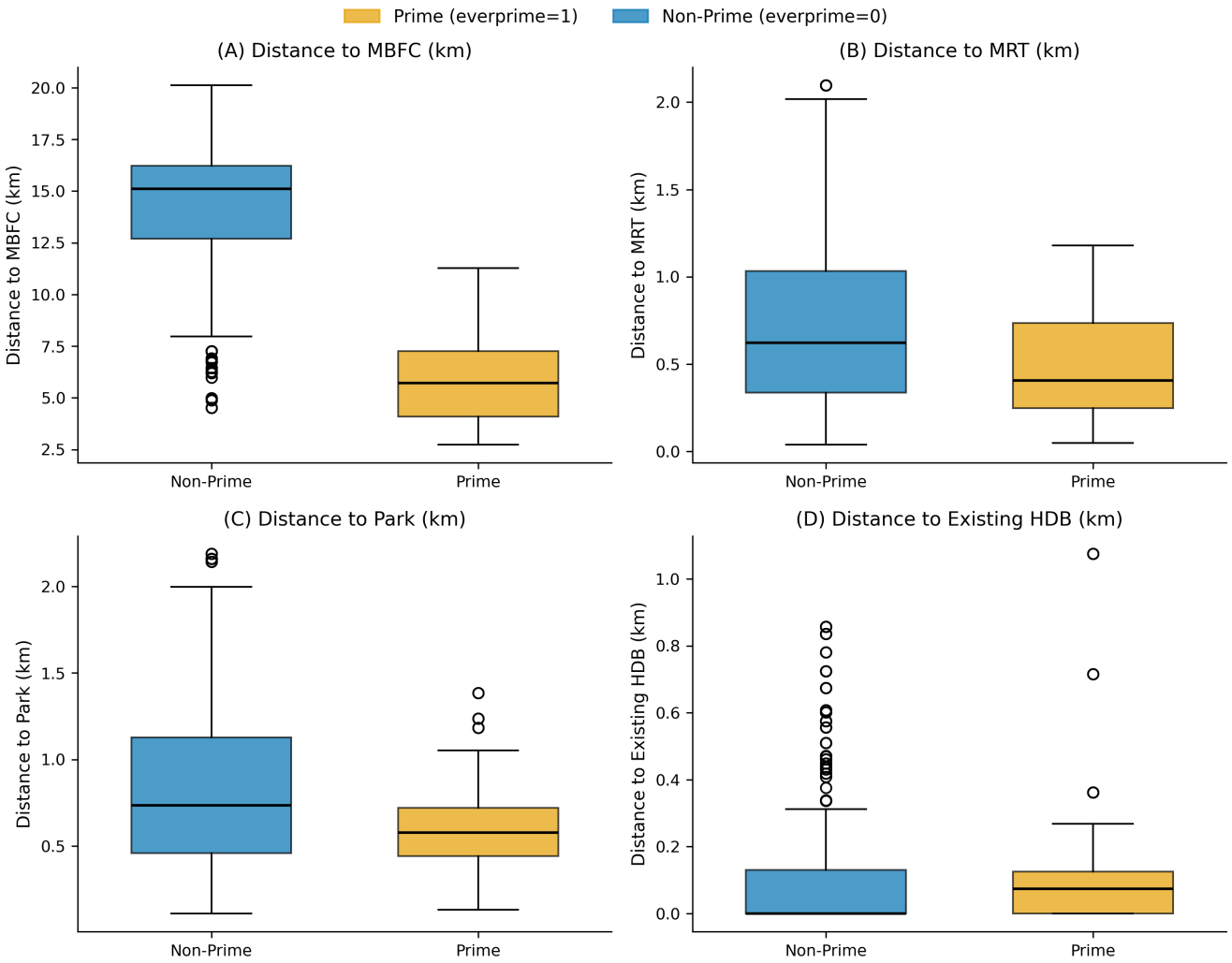

Appendix Figure A2. **Covariate Distributions by Prime Location Status.** *Panel A:* Distance to MBFC shows the starkest difference—Prime locations cluster within 4–7 km of the CBD while Non-Prime units are predominantly 12–16 km away, though some overlap exists in the 7–10 km range. *Panel B:* Distance to nearest MRT station shows considerable overlap, with Prime locations slightly closer (median 0.41 km vs 0.62 km). *Panel C:* Distance to parks exhibits substantial overlap between groups. *Panel D:* Distance to existing HDB developments shows near-complete overlap. *Implication:* While Prime and Non-Prime locations differ systematically in CBD proximity, the overlapping distributions for MRT access, park proximity, and existing HDB density support the overlap assumption (Assumption 2), indicating sufficient common support for counterfactual extrapolation in the difference-in-differences framework.

B Dataset

B.1 Data Collection Method

Geographic Data: We obtained the geographic coordinates of all BTO projects using the OneMap API, a government-provided geospatial service that offers programmatic access to Singapore's official mapping database.[3] For each project name, our code queried OneMap's search endpoint and retrieved the corresponding latitude–longitude pair from the authoritative national address registry. This automated procedure ensured high spatial accuracy and full consistency across all projects. Some project names did not perfectly match the identifiers in the geospatial database, resulting in missing coordinates in the automated retrieval process. For these cases, we manually verified the project locations and supplemented the dataset with the correct latitude–longitude values.

To construct distance-based features, we compiled multiple categories of point-of-interest (POI) datasets from publicly available GIS sources. These include MRT station exits, schools, parks, supermarkets, and major road networks, obtained in GeoJSON or KML format from agencies such as the Land Transport Authority (LTA) and Urban Redevelopment Authority (URA). We additionally incorporated manually curated coordinate lists for specific landmarks, such as major shopping malls and the Marina Bay Financial Centre (MBFC), as well as specialized school categories (SAP/GEP schools).

Using the project coordinates together with the POI feature sets, we computed the great-circle (Haversine) distance from each BTO project to the closest amenity within each category. For instance, the distance to "nearest MRT" is defined as the minimum Haversine distance between the project and all MRT station exit coordinates; similarly, distances to the nearest park, school, supermarket, or major road were calculated. Distances are expressed in kilometers.

This process yields a comprehensive set of spatial accessibility measures capturing urban connectivity, amenity proximity, and locational advantages for every BTO project in our dataset. The resulting spatial features are later used in both descriptive analysis and empirical modeling.

B.2 Dataset Cross Section

[3] https://www.onemap.gov.sg

Appendix Table A1. First Five Rows of Dataset (Part 1 of 6)

id	room	supply	demand	first_timer_rate	second_timer_rate	overall_rate	month	year	town
1511013	3-room	329.00	469	1.00	2.50	1.40	11	2015	Punggol
1511014	4-room	1021.00	1665	1.40	3.10	1.60	11	2015	Punggol
1511015	5-room	534.00	1345	1.50	8.50	2.50	11	2015	Punggol
1511023	3-room	79.00	198	2.00	3.70	2.50	11	2015	Bukit Batok
1511024	4-room	220.00	653	2.90	3.40	3.00	11	2015	Bukit Batok

Appendix Table A2. First Five Rows of Dataset (Part 2 of 6)

project_clean	wait_time_month	LAT	LON	dist_park_km	dist_supermarket_km	dist_hawker_km	dist_mrt_km	dist_sch
Waterfront I @ Northshore	57.00	1.42	103.90	0.86	0.39	1.03	0.28	
Waterfront I @ Northshore	57.00	1.42	103.90	0.86	0.39	1.03	0.28	
Waterfront I @ Northshore	57.00	1.42	103.90	0.86	0.39	1.03	0.28	
West Quarry @ Bukit Batok	42.00	1.35	103.74	1.67	0.16	0.33	1.27	
West Quarry @ Bukit Batok	42.00	1.35	103.74	1.67	0.16	0.33	1.27	

Appendix Table A3. First Five Rows of Dataset (Part 3 of 6)

dist_hdb_existing_km	dist_hdb_uc_km	dist_sap_km	dist_gep_km	dist_mbfc_km	dist_mall_km	min_price	max_price	scheme	prime_bina
0.00	0.00	5.54	5.55	15.86	0.25	173000.00	223000.00	–	0
0.00	0.00	5.54	5.55	15.86	0.25	277000.00	372000.00	–	0
0.00	0.00	5.54	5.55	15.86	0.25	377000.00	489000.00	–	0
0.00	0.00	4.47	4.54	15.17	0.28	161000.00	202000.00	–	0
0.00	0.00	4.47	4.54	15.17	0.28	272000.00	321000.00	–	0

Appendix Table A4. First Five Rows of Dataset (Part 4 of 6)

plus_binary	standard_binary	dist_orchard_km	5room_binary	cycle_max_price	cycle_total_supply	cycle_median_dist_mbfc	next_cycle_tot

0.00	0.00	15.04	1.00	369923.08	4968.00	12.45
0.00	0.00	15.04	1.00	369923.08	4968.00	12.45
0.00	0.00	15.04	1.00	369923.08	4968.00	12.45
0.00	0.00	11.20	1.00	369923.08	4968.00	12.45
0.00	0.00	11.20	1.00	369923.08	4968.00	12.45

Appendix Table A5. First Five Rows of Dataset (Part 5 of 6)

geometry	pc_gni	pc_gdp	ave_sora_mth	median_resale_price	cpi	sti_close	sti_volume	room_
POINT (35363.74941983441 44269.45613595494)	71283	76503	0.42	–	84.81	2.92	4935100	
POINT (35363.74941983441 44269.45613595494)	71283	76503	0.42	420000.00	84.81	2.92	4935100	
POINT (35363.74941983441 44269.45613595494)	71283	76503	0.42	446900.00	84.81	2.92	4935100	
POINT (17537.88363078804 37372.959881147515)	71283	76503	0.42	280000.00	84.81	2.92	4935100	
POINT (17537.88363078804 37372.959881147515)	71283	76503	0.42	402000.00	84.81	2.92	4935100	

Appendix Table A6. First Five Rows of Dataset (Part 6 of 6)

mature	prob_first	log_prob_first	everprime	everplus	postoct24	postnov21	postaug23	everprime_postnov21
0.00	1.00	0.00	0.00	0.00	0.00	0.00	0.00	0.00
0.00	0.71	-0.34	0.00	0.00	0.00	0.00	0.00	0.00
0.00	0.67	-0.41	0.00	0.00	0.00	0.00	0.00	0.00
0.00	0.50	-0.69	0.00	0.00	0.00	0.00	0.00	0.00
0.00	0.34	-1.06	0.00	0.00	0.00	0.00	0.00	0.00

C Causal Forest

C.1 Development of CF-DiD

The CF-DiD estimator builds on a rich econometric tradition addressing treatment effect estimation when selection into treatment depends on observables. Abadie (2005a) established the foundation by showing that difference-in-differences can be reweighted using propensity scores to recover treatment effects under conditional parallel trends—a weaker requirement than the unconditional version. This insight opened the door to semiparametric approaches that leverage covariate information to construct valid counterfactuals when treated and control groups differ systematically.

The subsequent development of Double/Debiased Machine Learning (DML) by Chernozhukov et al. (2015) provided a framework for incorporating flexible machine learning estimators into causal inference while preserving valid statistical inference. DML addresses the regularization bias inherent in machine learning predictions through sample splitting and orthogonalization, yielding $\sqrt{n}$-consistent estimates of low-dimensional causal parameters even when high-dimensional nuisance functions are estimated nonparametrically. This framework enabled researchers to move beyond restrictive parametric specifications without sacrificing the asymptotic properties required for hypothesis testing.

Causal forests, developed by Wager and Athey (2018) and generalized by Athey et al. (2019), adapt random forests to treatment effect estimation. A standard random forest constructs an ensemble of decision trees trained on bootstrap samples, averaging predictions to reduce variance. Causal forests modify the splitting criterion to maximize treatment effect heterogeneity across subgroups rather than minimizing prediction error, producing flexible nonparametric estimators of conditional average treatment effects. Crucially, the honesty property—using separate subsamples for tree construction and estimation—enables valid asymptotic inference.

Gavrilova et al. (2025) synthesize these advances into the CF-DiD framework. The causal forest learns the conditional expectation of outcomes given covariates among control units, capturing how observables predict outcome trajectories absent treatment. For treated units post-reform, this trained model imputes counterfactual outcomes, with treatment effects recovered as the residual. The key innovation is operationalizing Abadie's conditional parallel trends assumption through the flexibility of causal forests, permitting consistent estimation when treated and control units differ systematically in observable characteristics.

C.2 Feature Importance

Figure A3 displays variable importance from the outcome model. Distance to existing HDB (23.2%), room type (18.3%), and distance to CBD (15.4%) emerge as the strongest predictors, consistent with hedonic housing models emphasizing location and size as primary value drivers.

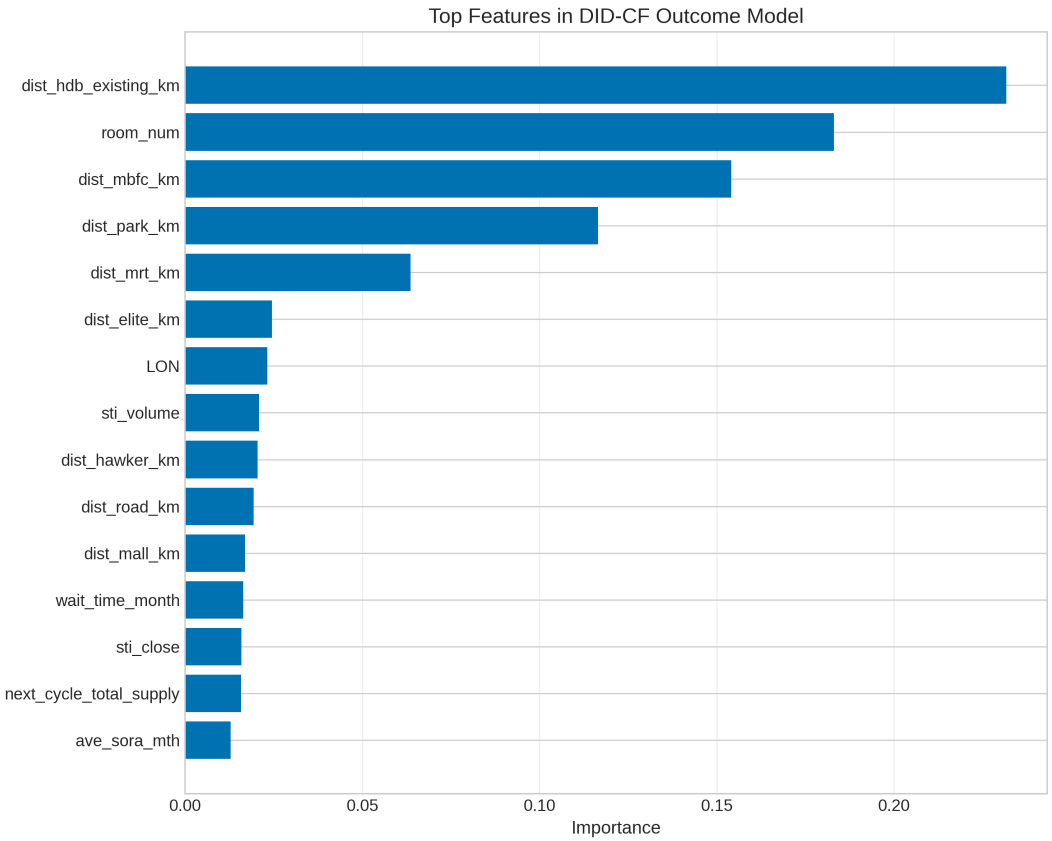

Appendix Figure A3. **Feature Importance in CF-DiD Outcome Model.** This figure displays the relative importance of covariates in predicting first-timer success probability, as measured by the random forest's mean decrease in impurity. *Interpretation:* (1) Location variables (distance to existing HDB, CBD, parks, MRT) dominate, explaining over 60% of predictive power; (2) Room type captures size-related demand variation; (3) Macroeconomic variables contribute modestly, reflecting time fixed effects absorbing aggregate trends. *Implication:* The outcome model appropriately captures hedonic housing value determinants, supporting the plausibility of counterfactual predictions.

References

Alberto Abadie. Semiparametric difference-in-differences estimators. *Review of Economic Studies*, 72(1):1–19, 2005a.

Alberto Abadie. Semiparametric difference-in-differences estimators. *The Review of Economic Studies*, 72(1):1–19, 2005b.

Susan Athey. Machine learning and causal inference for policy evaluation. In *Proceedings of the 21st ACM SIGKDD International Conference on Knowledge Discovery and Data Mining*, pages 5–6. ACM, 2015.

Susan Athey, Julie Tibshirani, and Stefan Wager. Generalized random forests. *The Annals of Statistics*, 47(2):1148–1178, 2019.

A. Colin Cameron and Douglas L. Miller. A practitioner's guide to cluster-robust inference. *Journal of Human Resources*, 50(2):317–372, 2015.

Victor Chernozhukov, Christian Hansen, and Martin Spindler. Valid post-selection and post-regularization inference: An elementary, general approach. *Annual Review of Economics*, 7(1): 649–688, 2015.

Victor Chernozhukov, Denis Chetverikov, Mert Demirer, Esther Duflo, Christian Hansen, Whitney Newey, and James Robins. Double/debiased machine learning for treatment and structural parameters. *The Econometrics Journal*, 21(1):C1–C68, 2018.

Cody Cook, Pearl Z. Li, and Ariel J. Binder. Where to build affordable housing? evaluating the tradeoffs of location. Working Paper 23-62, Center for Economic Studies, U.S. Census Bureau, 2023.

Department of Statistics Singapore. Key household income trends, 2024. URL https://www.singstat.gov.sg/find-data/search-by-theme/households/household-income/latest-data. Accessed: 2024.

Mi Diao, Delon Leonard, and Tien Foo Sing. Spatial-difference-in-differences models for impact of new mass rapid transit line on private housing values. *Regional Science and Urban Economics*, 67:64–77, 2017. doi: 10.1016/j.regsciurbeco.2017.08.006.

Andrew Ferdowsian, Kwok Hao Lee, and Luther Yap. Build-to-order: Endogenous supply in centralized mechanisms. Working Paper, 2025. URL https://ssrn.com/abstract=5085896.

Evelina Gavrilova, Audun Langørgen, and Floris T. Zoutman. Difference-in-difference causal forests with an application to payroll tax incidence in Norway. *Journal of Applied Econometrics*, 40(1):1–20, 2025. doi: 10.1002/jae.70001.

Judy Geyer and Holger Sieg. Estimating a model of excess demand for public housing. *Quantitative Economics*, 4(3):483–513, 2013.

Housing and Development Board. Helping first-time home buyers secure a bto flat, 2022. URL https://www.hdb.gov.sg/cs/infoweb/about-us/news-and-publications/publications/hdbspeaks/Helping-first-time-home-buyers-secure-a-BTO-flat. HDB Speaks.

Kwok Hao Lee and Brandon Joel Tan. Urban transit infrastructure and inequality. *Review of Economics and Statistics*, 2024. doi: 10.1162/rest_a_01442.

Kwok Hao Lee, Andrew Ferdowsian, and Luther Yap. The dynamic allocation of public housing: Policy and spillovers. *Working Paper*, 2024.

Robert M. O'Brien. A caution regarding rules of thumb for variance inflation factors. *Quality & Quantity*, 41(5):673–690, 2007.

Straits Times. Hdb resale prices rise for 22nd straight month pinnacle 4 room flat sells for record 1.228m, 2022. URL //www.straitstimes.com/singapore/housing/hdb-resale-prices-rise-for-22nd-straight-month-pinnacle-4-room-flat-sells-for-record-12

Neil Thakral. The public-housing allocation problem: Theory and evidence from pittsburgh. Working Paper, 2016a.

Neil Thakral. The public-housing allocation problem: Theory and evidence from pittsburgh. *Working Paper*, 2016b.

Stefan Wager and Susan Athey. Estimation and inference of heterogeneous treatment effects using random forests. *Journal of the American Statistical Association*, 113(523):1228–1242, 2018.

Daniel Waldinger. Targeting in-kind transfers through market design: A revealed preference analysis of public housing allocation. *American Economic Review*, 111(8):2660–2696, 2021. doi: 10.1257/aer.20190516.

Qiyao Zhou. Under control? price ceiling, waiting, and misallocation: Evidence from the housing market in china. Working Paper, University of Maryland, 2023. URL https://ssrn.com/abstract=4597461.